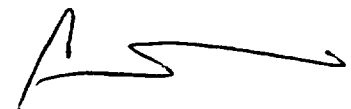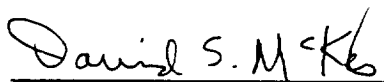# There's Iron in Them Thar Hills:
A Geologic Look at the Aristarchus Plateau as a
Potential Landing Site for Human Lunar Return

Dr. Cassandra R. Coombs
College of Charleston
SN
August 1, 1996

Dr. David S. McKay
Earth Science and Solar System Exploration Division
Space and Life Sciences Directorate

_____
Cassandra R. Coombs, Ph.D.

_____
David S. McKay, Ph.D.

There's Iron in Them Thar Hills:
A Geologic Look at the Aristarchus Plateau as a
Potential Landing Site for Human Lunar Return

Final Report

Prepared by: Cassandra R. Coombs, Ph.D.

Academic Rank: Assistant Professor

University & Department: College of Charleston
                                      Geology Department
                                      58 Coming Street
                                      Charleston, S.C.   29424

NASA/JSC

Directorate: Space and Life Sciences

Division: Earth Science and Solar
                                      System Exploration

JSC Colleague: David S. McKay, Ph.D.

Date Submitted: August 1, 1996

Contract Number: NAG 9-867

ABSTRACT

Lunar pyroclastic deposits are unique among lunar soils. Composed of very fine grained glass beads rich in Fe, Ti and Mg they yield unique spectral signatures. From the spectra two major classes and five subclasses of lunar dark mantling deposits have been identified. Recent work by me and others has shown that the larger regional deposits are more numerous, extensive, thicker, and widely distributed than previously thought, leading us to suggest that they would make ideal resource feedstock for future lunar surface activities. Returned sample studies and the recently collected Galileo and Clementine data also corroborate these findings. Recent planning for return to the Moon indicates that large cost savings can result from using locally produced oxygen, and recent JSC laboratory results indicate that iron-rich pyroclastic dark mantling deposits may be the richest oxygen resource on the Moon. My earlier work demonstrated that instead of using regolith, bulk lunar pyroclastic deposits are better suited for beneficiation as they are thick (10's m's), unconsolidated, fine-grained deposits. In addition, the lack of rocks and boulders and the typically flat to gently rolling terrain will facilitate their mining and processing. In preparation for the Human Lunar Return (HLR) I have characterized the Aristarchus Plateau (24°N 52°W) as a potential landing site for an in-situ resource utilization (ISRU) demonstration. The geologic diversity and large volume of Fe-rich pyroclastic material present at the Aristarchus site make it an ideal target for extracting O_2, H, and halogens. This paper (1) describes the current understanding of the geology of Aristarchus plateau; (2) describes the resource potential of the Aristarchus plateau ; and (3) presents several candidate landing sites on the plateau for future lunar activities.

There's Iron in Them Thar Hills:
A Geologic Look at the Aristarchus Plateau as a
Potential Landing Site for Human Lunar Return

INTRODUCTION

The NASA Strategic Plan calls for the US to open the space frontier by exploring, using, and enabling the development of space and to expand the human experience into the far reaches of space. [1]. More specifically, Goal 2 of the Human Exploration and Development of Space (HEDS) Enterprise calls for the U.S. to Explore and settle the Solar System [2]. As part of this, NASA is studying a small return mission to the Moon. This mission will be driven by more than pure science. The currently planned mission is focused on in-situ resource utilization and demonstration. However, much good science will accompany the mission. The location of the lunar base at a geologically interesting site such as Aristarchus will permit the investigation of the composition and mode of emplacement of basin ejecta, the impact cratering process, the nature and origin of crater rays, the formation of sinuous rilles, and the compositions and eruption styles of a variety of mare basalt units in the process of characterizing and defining the pyroclastic deposits in situ.

This study is a compilation of both orbital and Earth-based photographic and remote sensing observations. It began in support of NASA's Human Lunar Return mission. This past year NASA Administrator Dan Goldin requested that a feasibility study be conducted to return humans to the Moon. To be viable, this mission must not only return humans to the Moon but provide something new. That something new is technology. For the first time in history, this mission will investigate the potential for generating needed O_2 and He and other resource materials from another planetary surface, in this case, the lunar dark mantling deposits. Aristarchus is a site that is not only geologically interesting, but one that can provide an added benefit - resources. Careful evaluation of the returned Apollo sample data and imagery combined with the recent Clementine UV/VIS data confirm the resource potential at Aristarchus.

BACKGROUND

The Aristarchus Plateau is located in central northeastern Oceanus Procellarum on the lunar nearside (25°N 52°W). For years the Aristarchus Plateau has been a subject of interest to lunar scientists. It is one of the most geologically diverse regions for its size on the lunar surface. Recognized early in the Apollo days as being unique, it became an early candidate Apollo landing site when early site selection discussions stressed the need for geologic diversity and traverse distance.

The plateau is geologically diverse. Its surface is riddled with impact craters and secondary crater chains, volcanic constructs and pyroclastic deposits as well as many sinuous rilles and scarps (Figure 1). Among the geologic features are a blanket of anomalously red dark mantling material; the densest concentration of sinuous rilles as well as the Moon's largest lava channel, Schröter's Valley; apparent volcanic vents, volcanic sinks or depressions, volcanic domes; mare materials of various ages and colors; one of the freshest large craters with ejecta of varying unique colors and albedos; and other large craters in different states of flooding and degradation [3]. In addition to these geologic features, the three best authenticated lunar transient phenomena were observed emanating from the plateau area, which may or may not be due to presence of KREEP-rich materials in the region. Previous work by [4] and [5] suggested that pyroclastic deposits would make an ideal lunar base site. Past attention has focused on the production of H_3 as a nuclear fusion fuel and oxygen propellant [6,7,8,9].

What are pyroclastic deposits?
Lunar pyroclastic deposits are very smooth, low albedo (0.079 - 0.096:[10]) units that mantle and subdue underlying terrain. First found as whole and broken glass beads at Apollo 15, numerous classes of glass beads are now recognized in the returned Apollo sample collection. On the Apollo 17 mission orange glass beads and their quench-crystallized equivalents were identified at Station 4, Shorty Crater. Interpretations of their origin have swayed from (1) vapor condensates [11,12], (2) impact melt ejecta from large impacts which had penetrated to more mafic material at depth [13,14]; (3) splash droplets from impacts into lava lakes [15] or (4) pyroclastic material [16,17,18,19,20,21]. The latter, explosive volcanic origin is now commonly accepted for the well studied Apollo 17 and Apollo 15 returned glass beads and partially devitrified spherules. Recent studies have also demonstrated that explosive volcanism is responsible for the formation of the other dark mantle deposits on the lunar surface (e.g., 22,23,24,25,26).
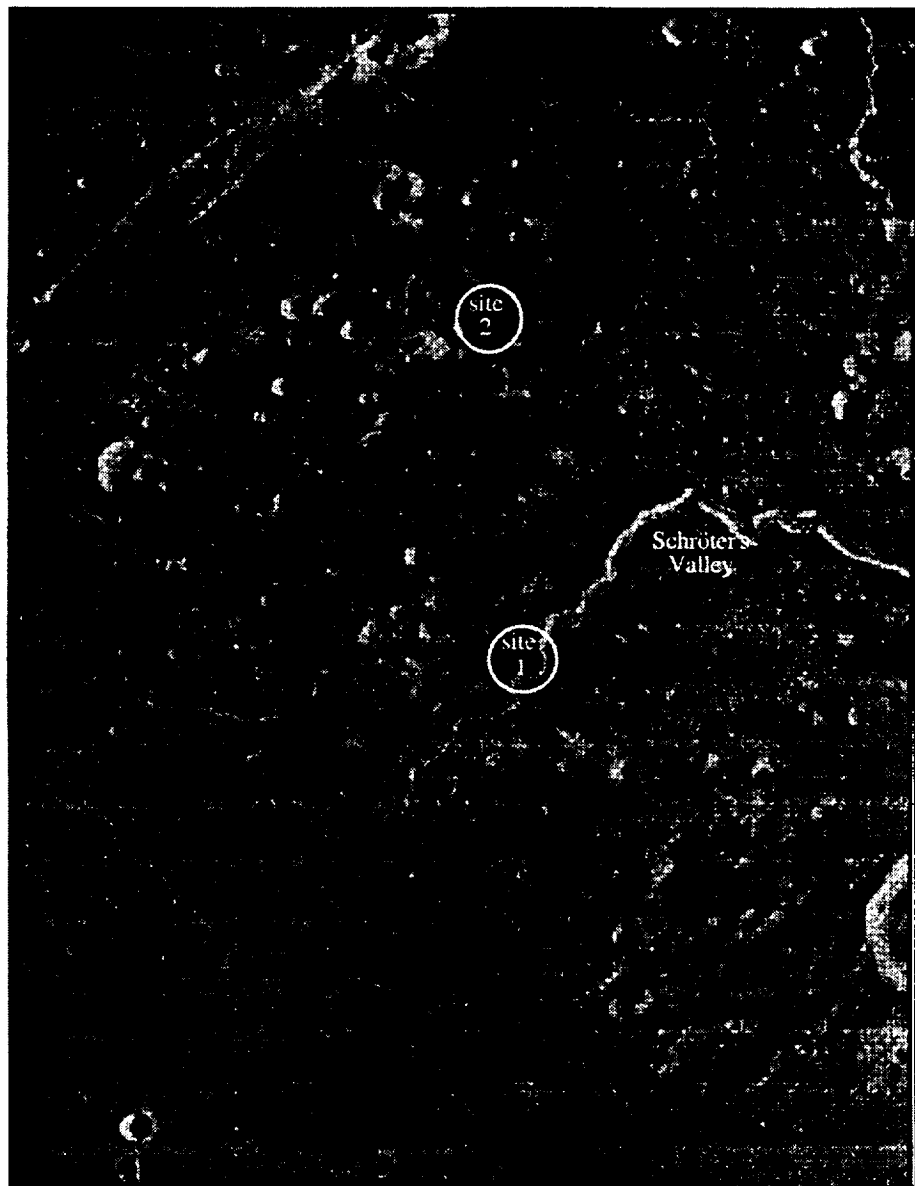

Figure 1: Lunar Orbiter IV photograph of the Aristrarchus Plateau. The circles denote the suggested landing sites. Each is approximately 10 km in diameter.

Modeling by Coombs and Hawke, Hawke et al., and Coombs [4,22,24] has demonstrated the nature and method of emplacement of the explosive volcanic materials. Two different methods are thought to be responsible for these dark mantle materials, based on their distribution and spectral signatures. Work by Gaddis et al., Coombs, and Hawke et al. [23,24,25] and others has demonstrated that regional pyroclastic deposits differ from localized dark-mantle deposits in that they typically cover several thousand square kilometers and were emplaced as a result of strombolian-type or continuous eruption column activity. The localized deposits, on the other hand are, are much smaller in that they are generally less than 250 km to around 550 square kilometers and were emplaced by a more short-lived eruption mechanism like the terrestrial vulcanian eruptions. See [4, 22-26] for more specific information.

DATA

Multiple data sets were used for this preliminary site study. Among them are, Apollo 15 Hasselblad and Metric Mapping Camera images, Lunar Orbiter IV and V panchromatic frames, Clementine multispectral data in the UV/VIS range, ground-based telescopic spectra in the UV/VIS to near-IR, orbital geochemistry and ground-based radar.

Imagery
Hand-held Hasselblad photos from the orbiting Apollo 15 Command Module were used as a cursory tool to locate the pyroclastic deposits on the Plateau. Close inspection of the Apollo 15 metric mapping camera frames revealed sufficient detail to pinpoint potential resource areas, volcanic source vents and rilles, and ejecta blocks in the study areas. In addition, the southward looking metric frames provided a low sun-angle view for more clearly distinguishing feature morphology. The incident sun angle ranges between 10-12° on the frames used. The Lunar Orbiter IV and V frames provided a different view for the study areas. With a spatial resolution of approximately 10 km, and a different lighting angle than the mapping camera the Orbiter frames nicely complement the metric mapping camera images and provide a more effective concept of distance and scale.

Clementine
Following the return of Clementine multispectral data McEwen et al. [27] developed a rudimentary mosaic of the Aristarchus Plateau soon after the Clementine data were received (Figure 2). I used their mosaic as a base for this study. A 30 km by 40 km subset of these data were extracted for closer analysis and assistance with site identification. McEwen et al. [27] examined the initial Clementine data for the Aristarchus region. They mosaiced more than 500 images in three spectral bands using the UV/VIS data; 415 nm, 750 nm, 1000 nm. To create a color ratio image, the 750/415-nm ratio image was assigned to the red channel, the 750/1000-nm ratio image to the green channel and the 415/750-nm ratio image to the blue filter (Figure 3). Most striking in this RGB image are the pyroclastic deposits which are a distinct red and red-orange. The blue areas in the image denote lobes of highland material extending asymmetrically west-northwest of the crater Aristarchus for 75-100 km. This distribution is consistent with previous studies [28, 29]. The yellowish areas in the image correspond to late stage ejecta removed from the crater rim which expose fresh mare basalt. The purplish or reddish units correspond to the red or blue mare units. Given the expected excavation depth of 1/3 - 1/10 the crater diameter, McEwen et al. [27] estimate the pyroclastic mantling thickness at between 10-30 m.

Ground-based spectra
Many spectral studies have been conducted of the Aristarchus region. Coombs[24] and Hawke et al. [25] looked at the localized pyroclastic deposits on the plateau. Ground-based spectra collected of this area indicate an additional Fe-bearing soil component. The spectra are broader and exhibit a longer-wavelength absorption band than the Taurus-Littrow dark mantle deposit. In addition, this higher Fe content helps to maintain the low albedo of these deposits.
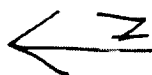
Figure 2: Clementine multispectral mosaic of the Aristarchus Plateau. Red and red-orange areas denote pyroclastic materials where we hope to process O_2 and He. Modified from [27]. Composed of three band ratios: 750/415-nm (red), 750/1000-nm (green), 415/750-nm (blue).

UV/VIS spectra collected from different areas on the plateau indicate a high Fe, moderate Ti composition (Figure 3, right). In particular, the higher resolution spectra presented by Hawke et al. [30] were collected over 120 channels versus the previous 24 channel spectra presented by Pieters et al. [31]. The 1991 spectra have a much improved spectral sampling and slightly enhanced resolution that can be used to identify mineral absorption features that were previously undetectable in the lower resolution data.

Near-infrared (near-IR) spectra for regional pyroclastic deposits presented by Gaddis et al. [23] were divided into two distinct classes. Regional Class 1 spectra exhibit broader, longer-wavelength absorption bands than those that can be attributed to just pyroxenes in mare or highland soils. This spectral signature suggests that an additional Fe-bearing soil component is present to modify the 1-μm band and maintain the low albedo of the materials observed. This finding is consistent with the presence of Fe^{2+}-bearing volcanic glass-rich mantling deposits on the Plateau and is supported by all available spectral evidence [23,24,25,30, 32]. The pyroclastic deposits atop the Aristarchus plateau fall into this category (Figure 3). Another pyroclastic mantling deposit within this spectral subclassification is a fairly large deposit just southwest of Mare Humorum.

Figure 3: UV/VIS spectra collected from Mauna Kea by [30] for three different lunar dark mantle deposits with potential for resource extraction and utilization. Left spectra are near-infrared spectra from the Aristarchus Plateau [32]. Right spectra are in the UV/VIS range from (a) Taurus Littrow (b)Sulpicius Gallus (c)Aristarchus Plateau [30].
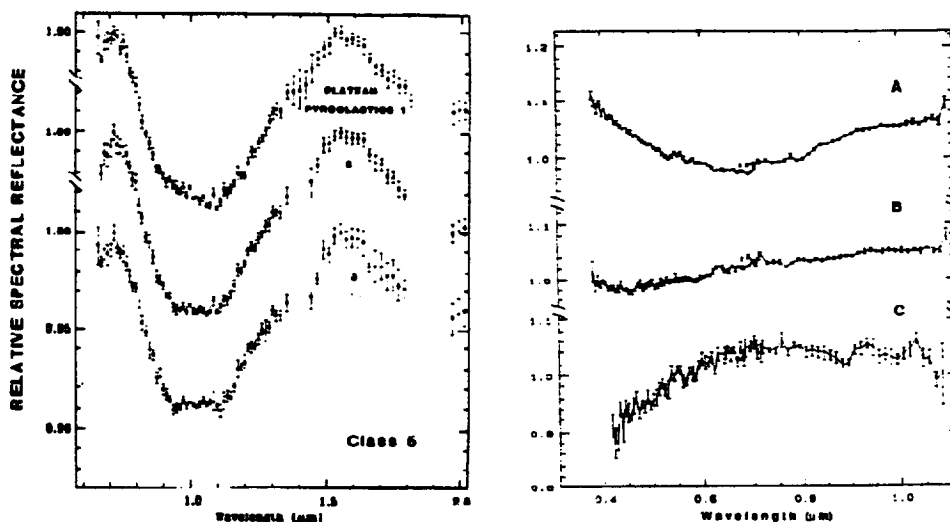
Regional Class 2 spectra on the other hand have signatures nearly identical to the Taurus-Littrow dark mantle deposit. Each of these deposits bears a spectral signature indicating a predominance of ilmenite-rich black spheres similar to those returned from the Apollo 17 Station 4 site. Other deposits within this spectral class are Rima Bode, southern Mare Vaporum and southern Sinus Aestuum.

The Aristarchus Plateau has low 0.40/0.56-μm UV/VIS values and relatively high values in the near-IR (see Figure 3, left). The steep infrared continua, low albedo and very broad absorption centered longward of 1μm has been attributed to Fe^{2+}-bearing glass. as mentioned above [32]. These data are consistent with those presented in previous studies based on multispectral imagery and color-difference photography [32, 33, 34]. The strong Fe^{2+} absorption signature indicated by the Aristarchus spectra does not necessarily connote a dominate composition of black spheres and orange glass as collected at Apollo 17. Instead, work by Davies et al.[35] and Johnson et al. [36] suggest that the Aristarchus spectral signatures are indicative of the presence of glass-rich pyroclastic materials that are compositionally unrelated to those sampled by Apollo 17. Lucey et al. [32] argued that mixtures of Apollo 17 orange glass and black spheres would not yield spectra with the characteristics exhibited by the Aristarchus Plateau mantle deposits.

9-6

The large aerial extent of this deposit may protect parts of it from surface contamination by larger impact ejecta, limiting the effects of secondary impacts and lateral mixing. The relatively large thickness (10-30 m) of this deposit is deep enough that the smaller impact craters in the 10-100's m size range have generally not penetrated the dark mantle material and ejected or exposed subjacent blocky material. Perhaps, as previously suggested by Zisk et al. [33], the Aristarchus dark mantle materials are themselves covered with a thin layer of Aristarchus crater ejecta and fine grained highlands-rich materials that are masking the strong pyroclastic characteristic signature.

Orbital geochemistry

The Apollo 15 command module carried several geochemical experiments onboard including a gamma ray spectrometer, an X-ray fluorescence spectrometer, and an α-particle spectrometer [34]. The gamma ray spectrometer is used for detecting iron, magnesium, titanium, thorium and potassium. The X-ray fluorescence experiment investigated the aluminum, silicon and magnesium concentrations while the α-particle spectrometer measured radiation. The footprint for the Apollo 15 instruments was large and thus often overlapped adjacent geologic units impeding specific compositional analyses. However, when combined with other ground-based observations and the recent Clementine data they are very useful. The Apollo 15 data revealed an apparent depressed thermal neutron flux which has been attributed to high concentrations of KREEP and thorium. KREEP and thorium are thought to be associated with the Aristarchus crater and ejecta [36] and may provide an additional resource.

McCord et al. [34] reported that the values of iron, magnesium and titanium for the Aristarchus region are all above the Apollo 15 average (see Table 1) and the percentage of titanium present at Aristarchus (2.2%) is higher than in the mare materials to the west (2%) and in Mare Imbrium to the east (1.4%). These values led [33] to suggest that the titanium content in the mare and Plateau mantling materials may be even larger than indicated if ejecta from Aristarchus is low in titanium and thereby dilutes or masks the titanium concentration in those materials. Further, [33] suggested that the Aristarchus mantling materials are very similar to the high titanium orange glass present and collected at Taurus Littrow by the Apollo 17 astronauts. The X-ray fluorescence experiment obtained an Al/Si ratio of 0.3 ± 0.04 for a region north of Schröter's valley which is very similar to the returned lunar KREEP samples and mare materials at an average of about 0.39. Highlands materials on the other hand are much higher at around 0.54 [38, 39].

TABLE 1: Orbital Geochemical Results*

	Area	Fe(%)	Mg(%)	Ti(%)	Th (ppm)	K(ppm)
Aristarchus	39°W - 54°W ~17°N - 30°N	13.6	6.2	1.4	5.8	1700
Oceanus Procellarum	54°W - 81°W ~10°N - 30°W	9.6	4.9	2.2	6.9	2500
Mare Imbrium	15°W - 39°W ~22°N - 30°N	10.5	4.6	2.0	3.9	1700
Average Apollo 15	-	8.7	4.8	1.45	2.2	1230

*[after 33]

Ground-based radar

A radar survey of the Aristarchus Plateau region was completed by [33 and 40]. Dual polarization 3.8 cm maps for the Moon were acquired by Zisk et al. [33] with a spatial resolution of about 2 km. The most recent 70-cm maps of the Moon were acquired by Thompson [40] at a spatial resolution of about 3 km. Both of these radar image data sets were examined to provide additional information concerning the surface roughness, distribution, and thickness of the pyroclastic deposits. Their studies confirmed the lack of surface signal scatterers in the 1-50 cm size region over much of the plateau. This scarcity of surface signal scatterers is evidenced by the dark radar returns, or darker regions in the images. Figure 4 illustrates the dark radar return from the Aristarchus Plateau and other regional pyroclastic deposits such as Rima Bode. The bright patches represent areas with high surface scatter, or large blocks of rock and lighter, more reflective materials. In addition, the high dielectric losses denoted by the low return suggest the presence of excess Fe and/or Ti.

Radar backscatter echoes are influenced by a combination of surface or subsurface roughness and the bulk dielectric properties of the target materials. For lunar observations, a circularly polarized energy wave is transmitted, and both senses of circular polarization are received. The echo with polarization orthogonal to that transmitted is referred to as polarized, since it corresponds to the return expected from a flat reflecting plate. The echo with polarization identical to that transmitted is referred to as depolarized. The polarized echo is assumed to be the sum of a quasispecular component, due to scattering from facets large with respect to the radar wavelength, and a diffuse return or multiple scattering among wavelength scale objects, either on the target surface or within perhaps 100 radar wavelengths of the surface. The depolarized return is dominated by the diffuse echo. At low angles of incidence (near to nadir viewing geometry), the quasispecular echo will dominate the polarized return, and is very sensitive tonal changes in regional slope or roughness on horizontal scales of 10-100 m.
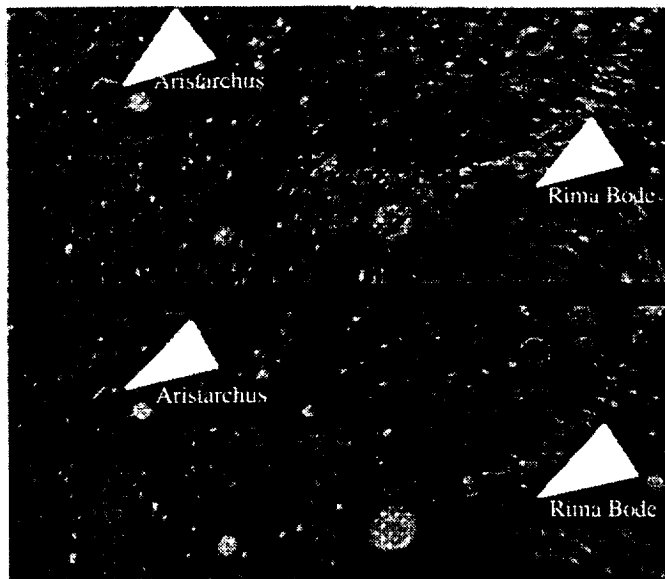

Figure 5: 70-cm radar images of the Aristarchus Plateau and Rima Bode regions (arrows). (a) polarized (b) depolarized. FOV = 2.6°-35.0°N, 62.5°W - 11.4°E.

Spudis and Davis [28] demonstrated that the Aristarchus regional pyroclastic deposit is deeper than the Rima Bode deposit based on the 70-cm radar returns. Results of early analyses indicate that the greatly attenuated polarized and depolarized returns from the Aristarchus Plateau imply a smooth-surfaced, fine grained, highly lossy mantling deposit [33, 40]. The incident 70-cm radar energy is assumed to penetrate the loose pyroclastic debris, traverse the voids within the deposit, and return from the interface between the highlands regolith and mantle [28]. Zisk et al. [33] proposed a

mantle depth of 5-20 m for the Aristarchus Plateau. More recently, McEwen et al. [27] suggested a mantle depth of between 10-30 m based on crater penetration depth/diameter ratios.

Eclipse temperature maps can be generated from infrared observations of the lunar surface. These data and resultant maps can be used to identify lunar surface units with distinct thermal properties. Varying rock surfaces such as large blocky boulders have a different signature than the finer grained regolith fraction. Infrared eclipse temperatures have been measured in the 11 μm band with resolutions of 10-15 km [41, 42]. Once totally eclipsed, significant temperature differences are present between points on the surface. These differences are related to a variety of variables including, albedo, slope, solar illumination, eclipse geometry, and initial temperature of the full moon. The main driving factor in the temperature differentials are due to thermo-physical parameters such as rock/grain size and distribution as well as the thermal inertia of the material [31, 41].

At full moon, the lunar surface brightness temperatures are affected and controlled by two dominant factors, insulation and surface albedo. As with a light sandy beach, directly illuminated areas are warm and those surfaces in shadow or pointing away from the sun are relatively cool. Similarly, the dark mare will tend to be warmer than the lighter highlands, as a black-top road becomes hotter than a lighter concrete road surface. During times of eclipse, planetary surface temperatures cool rapidly except where high-conductivity paths trap heat in a 'sink', or a large, exposed rock.

The Aristarchus plateau IR-eclipse temperatures fell below those for similarly low albedo areas elsewhere on the surface. {31] reports the Aristarchus Plateau several degrees cooler than adjacent areas, setting it apart from other low albedo areas. This low return can only be attributed to the lack of large blocks of rock (>10 cm; [40].

GEOLOGY OF ARISTARCHUS

The dark mantle material present in the Aristarchus area is superposed on pre-Imbrian and Imbrian materials. The pyroclastic deposit covers 37,400 km^2. The mare materials present in the vicinity of the Plateau are thought to be part of the Harbinger formation [44]. The pyroclastic deposits are of Eratosthenian and Copernican age (Figure 4).

Domes present just north of Schröter's Valley are thought to be volcanic. Image analysis for this study and previous maps (e.g., 44, 45) indicate the presence of probable source craters atop several of the domes. Craters Herodotus D and Aristarchus R (see map) are flanked by lava flows and smooth dark mantle material. Additionally, Schröter's Valley and the small parasitic rille on the interior floor are Copernican in age.

Mare materials once embayed the highlands material present on the surface of the Aristarchus region. Constructive volcanism began in the region forming the plateau and volcanic domes through the Copernican Era. Lava flows were accompanied by sporadic explosive eruptions in many different locations around the plateau. This activity was accompanied by tectonic uplifting and rifting along the north and northwestern edge of the plateau giving rise to its 1° westward downslope and 100 m rise above the adjacent western boundary with Oceanus Procellarum. Perhaps spawned by the Aristarchus impact event, Cobra Head formed in association with explosive volcanic eruptions that mantled the plateau.

The Aristarchus plateau is an uplifted region extending north-northwest of the craters Aristarchus and Herodotus. Recent Clementine altimetry data show the northwest edge of the plateau sitting nearly 100 m above the adjacent mare terrain in Oceanus Procellarum. The plateau is covered with a relatively thick blanket of pyroclastic (fire-fountain) material that most likely emanated from Cobra Head and other smaller vents nearby. The largest and most conspicuous volcanic source crater on the lunar surface. It is believed to be the source for Schröter's Valley. Aristarchus crater

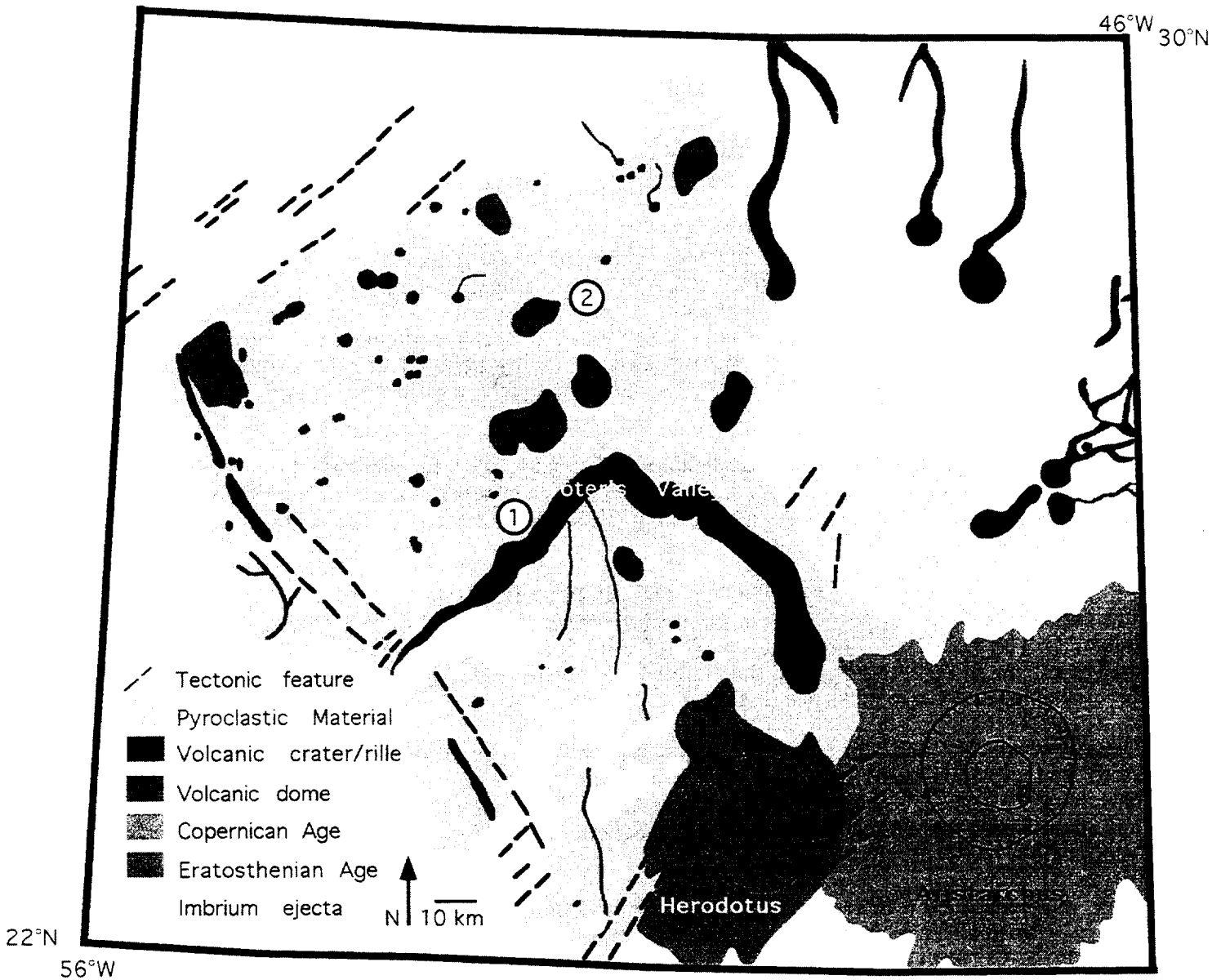Figure 4: Simplified Geologic Map of the Aristarchus Region

Figure 4: Simplified geologic map of the Aristarchus Plateau region. Note relationship and distribution of volcanic vents, domes and rilles on the plateau.

is a Copernican aged impact crater (40 km diameter) which should expose both Imbrian ejecta and pre-Imbrian material. Herodotus crater is a flooded, Imbrian-aged impact crater (35 km diameter) located just west of Aristarchus. The floor of Oceanus Procellarum is Eratosthenian in age. This mare deposit lies adjacent to the western edge of the Aristarchus plateau. Spectrally, this unit is a very 'blue', low albedo unit in contrast to the bright 'red' spectral nature of the Aristarchus Plateau.

RESOURCE POTENTIAL

These two candidate sites are particularly well suited for in-situ resource generation and utilization based on their spectral signatures and depth of material. In-situ resources are resources existing in the environment, in the atmosphere or at the surface of a planet or satellite. To date, humans venturing into space have relied almost exclusively on equipment and supplies carried from Earth. This strategy is certainly appropriate for operations in Earth orbit, or for stays of a few days on the surface of the Moon. However, the ability to effectively utilize local resources, to "live off the land," will prove vital for long term human habitation of the Moon and planets.

Some resources, *i.e.* solar energy for power and the martian atmosphere for aerobraking, will be exploited by the next generation of robotic spacecraft. Other resources, such as use of the local soil for radiation shielding, will be important to support a long-term human presence. Still others, notably export of helium-3 for fusion reactors on Earth, may only become feasible in the distant future.

Extraction of lunar oxygen for rocket propulsion is a key example of in-situ resource utilization which will directly support a long-term human presence on the Moon. This is because one of the largest elements in any rocket is the oxygen required to burn the fuel. Nearly 90% of the propellant mass of a liquid hydrogen-liquid oxygen rocket is oxygen. Locally-produced oxygen for rocket propulsion promises by far the greatest cost and mass saving of any in-situ lunar resource [46].

Over twenty different processes have been proposed for oxygen production on the Moon [47]. One of the simplest and best-studied of these processes involves the subsolidus reduction of ferrous iron (Fe^{2+}) in lunar minerals and glass using hydrogen gas. This method of oxygen production is a two-step process. Ferrous iron (as FeO) is first reduced to metal, and oxygen is liberated to form water:

$$FeO + H_2 \rightarrow Fe + H_2O$$
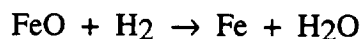
The water is then electrolyzed as a second step, with hydrogen recycled to the reactor and oxygen liquefied and stored.

Recent experiments on lunar materials and terrestrial analogs allow an assessment of the various proposed feedstocks for lunar oxygen production. Materials which have been proposed and/or tested include ilmenite, basalt, soil and volcanic glass. As the following discussion illustrates, some reacted better than others.

Ilmenite
Most previous work on lunar resources has focused on ilmenite ($FeTiO_3$) as the feedstock for oxygen production [48]. Ilmenite occurs in abundances above 25 wt% in some lunar rocks. This mineral is easily reduced, and oxygen yields of 8-10 wt% may be achievable. However, experiments to date have invariably failed to completely segregate ilmenite from other mineral fragments, so that stoichiometric oxygen yield has not been realized.

Lunar oxygen production scenarios which rely exclusively on ilmenite require processing to separate the mineral. This is done to minimize the amount of material that must be heated in order to release oxygen. Processing of soil includes sizing and magnetic separation. Processing of rock requires an initial crushing step. Thus, use of ilmenite alone for lunar oxygen production will involve high energy investments for feedstock preparation.

Basalt
The first experiments to extract oxygen from lunar material utilized high-titanium basalt 70035 [49]. This sample, with an initial iron content of 14.35 wt%, produced from 3.2 to 4.6 wt% oxygen in hydrogen reduction experiments run at temperatures of 900-1050°C.

Soil
Oxygen can be produced from a wide range of unprocessed lunar soils [50,51]. Iron-poor highland soils yield the smallest amounts of oxygen, 1-2 wt%. Mare soils, especially iron-rich samples, produce as much as 3.6 wt% oxygen. The dominant Fe-bearing phases in lunar soil are the minerals ilmenite, olivine, pyroxene and impact glass. Each of these phases is a source of oxygen.

Oxygen yield for lunar soils is strongly correlated with initial iron content [50,51]. Therefore it is possible to assess the potential for oxygen production at any location on the Moon for which the soil's Fe concentration is known. On a global scale, iron abundances in the near surface has been estimated from data returned by spacecraft. Iron was one of several elements measured from orbit during the Apollo 15 and 16 missions, using gamma ray spectrometry [52]. These data cover approximately 20% of the lunar surface, with spatial resolutions of around 100 km.

An improved gamma ray spectrometer is manifested on the Lunar Prospector mission, selected for flight in NASA's Discovery program [53]. This spacecraft, to be placed in a polar orbit, will provide geochemical data for the entire lunar surface. The spectrometer's spatial resolution will again be approximately 100 km.

A technique for iron assessment based on orbital multispectral imaging has recently been developed [54]. This method correlates iron abundance to a parameter derived from reflectance values at 750 and 900 nm. The authors use data from the Clementine spacecraft to map iron abundances across nearly the entire lunar surface. The spatial resolution of the initial study is 35 km. Clementine data, however, can support identification of iron-rich regions as small as a few hundred meters across at any location on the Moon.

Volcanic Glass
The optimum feedstock for production of lunar oxygen and other volatiles may be volcanic glass [26]. At least 25 distinct glass compositions have been identified in the Apollo sample collection [55]. The iron- and titanium-rich species, represented by the isochemical black and orange glasses from the Apollo 17 landing site, have demonstrated the highest oxygen yields of any lunar sample, approaching 4.5 wt% [50,51]. These samples are uniformly fine-grained, offering a feedstock which reacts rapidly and can be used with little or no processing prior to oxygen extraction.

Extensive areas of the lunar surface covered by volcanic glass have been delineated using Earth-based data and Apollo orbital photography [23]. Clementine multispectral imagery has recently been employed to determine the precise extent and estimate the thickness of one widespread deposit, that of the Aristarchus plateau [27].

POTENTIAL LANDING SITE(S)

Two potential landing sites were selected based on analysis of the early Apollo data and the more recent Clementine data. The pyroclastic sites were identified based on their low albedos, dark radar return signatures, and association with what appears to be volcanic vents and in some cases sinuous lava channels. Table 2 summarizes the features present within (1) 10 km radius and (2) 100 km radius of the two potential sites. See Figures 1 and/or 4 for locations.

Table 2: Candidate Landing Sites on Aristarchus Plateau

Site	Features within 10 km radius	Features within 100 km radius
Site 1 25° 25' N 52° 20' W	*Location/Site Description:* North rim of Schröter's Valley - low albedo - low radar return Pyroclastic material covers entire area - vents present - local area estimate of deposit ~170km^2 - potential volume ~1700 - 5100 km^3 - largest crater ~5 km diameter - access to Schröter's Valley - hummocky area, underlain by Imbrian ejecta *Characteristic Features Present:* - crater chains present - good view across Schröter's Valley for stratigraphic assessment and view of parasitic rille on floor of Schröter's Valley - very near volcanic dome material	*Location/Site Description:* Same as for 10 km and, *Characteristic Features Present:* Access to mare material in Oceanus Procellarum - hummocky terrain - access to northern domes
Site 2 27° 50' N 51° 20' W	*Location/Site Description:* East of Herodotus X - very low albedo - very low radar return - local area estimate of deposit >800km^2 - potential volume ~4000 - 24000 km^3 *Characteristic Features: Present* - access to Herodotus X - probable pyroclastic source vents - access to small rille for stratigraphic analysis - several crater chains present , mantled with pyroclastic materials - relatively fresh craters with prominent rims (<100 m dia.)	*Location/Site Description:* Same as for 10 km *Characteristic Features: Present:* - access to Harbinger Mountains and other structural features to the north - access to probable volcanic vent chain and ridges - access to more rilles for stratigraphic analysis

REFERENCES

[1]   NASA Strategic Plan, 1996

[2]   HEDS Strategic Plan, 1996

[3]   Zisk S.H., C.A. Hodges, H.J. Moore, R.W. Shorthill, T.W. Thompson, E.A. Whitaker, and D.E. Wilhelms, "The Aristarchus-Harbinger Region of the Moon: Surface Geology and History from Recent Remote-Sensing Observations", The Moon, 17, p. 59-99, 1977.

[4]   Coombs C.R. and Hawke B.R., "Lunar pyroclastic deposits". GSA Abstracts with Program, p. 237, 1988.

[5]   Hawke B.R., C.R. Coombs, L.R. Gaddis, P.G. Lucey, and P.D. Owensby, "Remote sensing and geologic studies of localized dark mantle deposits on the Moon", Proc. Lunar Planet. Sci. Conf. 19th, pp. 255-268, 1989.

[6]   Kulcinski G.L., J.F. Santarius and L.J. Wittenberg. "Presentation at the 1st Lunar Development Symposium, 1986.

[7]   Kulcinski G.L. ed. "Astrofuel for the 21st Century. "College of Engineering, Univ. of Wisconsin, Madison, 20 pp.

[8]   Gibson M.A. and C.W. Knudsen, " Lunar oxygen production from ilmenite", In Lunar Bases an Space Activities of the 21st Century, W.W. Mendell, ed., pp. 543-550, 1985.

[9]   Simon M.C., "A parametric analysis of lunar oxygen production", In Lunar Bases and Space Activities of the 21st Century, W.W. Mendell, ed., pp. 531-541, 1985.

[10]   Pohn and Wildey, "Color Difference Albedo Map of the Moon", 1970.

[11]   Cavaretta G., R. Funiceileo, H. Giles, G.D. Nichols, A. Taddeuccci, J. Zussman, " Geochemistry of green glass spheres from Apollo 15", In The Apollo 15 Lunar Samples, Lunar Science Institute, pp. 202-203, 1972.

[12]   Quaide W. , "Provenance of Apennine Front regolith materials (abstract). In Lunar Science IV, Lunar and Planetary Institute, pp. 606-607.1973.

[13]   Carr M.H. and C.E. Meyer, "Chemical and petrographic characteristics of the regolith at the Apollo 15 landing site. In The Apollo 15 Samples, Lunar Science Institute, pp. 48-50, 1972.

[14]   Hussain L, "The Ar-Ar and cosmic ray exposure ages of Apollo 15 crystalline rocks, breccias and glasses", In The Apollo 15 Lunar Samples, Lunar Science Institute, pp. 374-376, 1972.

[15]   Roedder E. and P. Weiblen, "Origin of orange glass spherules in Apollo 17 sample 74220, EOS Trans. Amer. Geophys. Union, 54, pp. 612-613, 1973.

[16]   McKay D.S. and G. Heiken, 1973.

[17]   McKay D.S., U.S. Clanton, and G. Ladle, " Scanning electron microscope study of Apollo 15 green glass", Proc. 4th Lunar Sci. Conf., pp. 225-238, 1973.

[18]   Huneke J.C., F.A. Podesek, and G.J. Wasserberg, "An argon bouillabaisse including ages from the Luna 20 site", in Luna Science IV, Lunar Science Institute, pp. 403-405, 1973.

[19]   Carter J.L., E. Padovani, H.C. Taylor, "Morphology and chemistry of particles from Apollo 17 soils 74220, 74241 and 74801", EOS Trans Amer. Geophys. Union, 54, 582-584, 1973.

[20]   Reid A.M., J.L. Warner, W.I. Ridley, R.W. Brown, and G. Moreland, "Apollo 17 orange glass, Apollo 15 green glass and Hawaiian lava fountain glass, EOS Trans. Amer. Geophys. Union, 54, pp. 606-607, 1973.

[21]   Heiken G.H. and D. McKay, Abstracts and Program, Geol. Soc. of America Ann. Meeting, 1974.

[22]   Wilson L. and J. Head, "Ascent and eruption of basaltic volcanism on the Earth and Moon", J. Geophys. Res., 78, 2971-3001, 1981.

[23]   Gaddis L.R., C.R. Pieters, B.R. Hawke , " Remote sensing of lunar pyroclastic mantling deposits", Icarus, 61, 461-489, 1985.

[24]   Coombs C.R., "Explosive Volcanism on the Moon and the Origin of Lunar Sinuous Rilles and their Terrestrial Counterparts", Ph.D. Dissertation, U. Hawaii, 256 p., 1989.

[25]   Hawke B.R., Coombs C.R., Gaddis L.R., Lucey P.D., Owensby P.D., "Remote sensing and geologic studies of localized dark mantle deposits on the Moon." Proc. 19th Lunar and Planetary Sci. Conf.", pp. 255-268, 1989.

[26]   Hawke B.R., Coombs C.R. and Clark B.E. "Pyroclastic deposits: An ideal lunar resource", Proc. 20th Lunar and Planetary Sc. Conf., pp. 249-258, 1990.

[27]   McEwen A.S., M.S. Robinson, E.M. Eliason, P.G. Lucey, T.C. Duxbury, P.D. Spudis, "Clementine Observations of the Aristarchus Region of the Moon", Science, v. 266, pp. 1858-1861, 1994.

[28]   Spudis P.D. and P. Davis, Lunar and Planetary Science Conf., 1991.

[29]   Davis P. and P.D. Spudis, "Global petrologic variations on the moon: A ternary-diagram approach, Proc. 17th Lunar Planet. Sci. Conf., in J. Geophys. Res., 92, 1987.

[30]   Hawke B.R., C.R. Coombs, B.A. Campbell, P.G. Lucey, C.A. Peterson, S. Zisk, "Remote Sensing of Regional Pyroclastic Deposits on the North Central Portion of the Lunar Nearside", Proc. 21st Lunar and Planetary Sci., pp. 377-389, 1991.\

[31]   Pieters CM, T.B. McCord, S.H. Zisk, and J.B. Adams, "Lunar black spots and the nature of the Apollo 17 area", J. Geophys. Res., 78, pp. 5867-5875, 1973.

[32]   Lucey P.G., B.R. Hawke, C.M. Pieters, J.W. Head, and T.B. McCord, "A compositional study of the Aristarchus region of the Moon using near-infrared reflectance spectroscopy", Proc. 16th Lunar and Planetary Sci. Conf., pp. D344-D354, 1986.

[33]   Zisk S.H., C.A. Hodges, H.J. Moore, R.W. Shorthill, T.W. Thompson, E.A. Whitaker, D.E. Wilhelms, ": The Aristarchus-Harbinger region of the Moon: Surface geology and history from recent remote sensing observations", The Moon, 17, pp. 59-99, 1977.

[34] McCord T.B., R.N. Clark, B.R. Hawke, L.A. McFadden, P.D. Owensby, C. M. Pieters, and J.B. Adams, "Moon: Near-infrared spectral black spots and the nature of the Apollo 17 landing area", J. Geophys. Res., 78, pp. 5867-5875, 1981.

[35] Davies D.W., T.V. Johnson, and D.L. Matson, "Lunar multispectral mapping at 2.26 microns: First results", Proc. 10th Lunar and Planetary Science Conf., pp. 1819-1828, 1979.

[36] Johnson T.V., J.A. Mosher, and D.L. Matson, "Lunar spectral units: A northern hemispheric mosaic", Proc. 8th Lunar and Planet. Sci. Conf., pp. 1013-1028, 1977.

[37] Metzger A.E., J.I. Trombka, R.C. Reedy, J.R. Arnold, "Element concentrations from Lunar Orbital Gamma-Ray Measurements", Proc. 5th Lunar and Planetary Science Conf. Suppl. 5, Geochim. Cosmochim. Acta 2, pp. 1067-1078, 1074.

[38] Adler I, J. Trombka, J. Gerard, P. Lowmann, R. Schmadebeck, A. Blodgett, E. Eller, L. Yin, P. Gorenstein, and Bjorkholm, " Apollo 15 Geochemical X-ray Fluorescence Experiment: Preliminary Report", Science, pp. 436-440, 1972.

[39] Malin M.C., "Lunar red spots: Possible pre-mare Materials", Earth Planet. Sci. Letters, 21, pp. 331-341, 1974.

[40] Thompson T.W., "High resolution lunar radar map at 70-cm wavelength", Earth Moon Planets, 37, pp. 59-70, 1987.

[41] Shorthill R.W. and J.M. Saari, "Non-uniform cooling of the eclipsed moon: A list of thirty prominent anomalies, Science, 50, pp. 210-12 1965;

[42] Shorthill R.W., "The Infrared Moon: A Review", In Lucas, ed., "Thermal Characteristics of the Moon", Progress in Astronautics and Aeronautics, 28, 3-49, MIT Press. 1972.

[43] Shorthill R.W., "Infrared Atlas Charts of the Eclipsed Moon", The Moon, 7, 22-45, 1973.

[44] Moore H.J., "Geologic Map of the Seleucus Quadrangle of the Moon", U.S. Geol. Survey, Geol. Inv. Map I-527, 1967.

[45] Moore H.J., "Geologic Map of the Aristarchus Quadrangle of the Moon", U.S. Geol. Survey, Geol. Inv. Map I-465, 1965.

[46] Joosten, B. K., and L. A. Guerra, "Early lunar resource utilization: A key to lunar exploration", AIAA Space Programs and Technol. Conf. Paper 93-4784, American Institute of Aeronautics and Astronautics, Washington, D. C., 1993.

[47] Taylor, L. A., and W. D. Carrier III, "The feasibility of processes for the production of oxygen on the Moon", in Engineering, Construction and Operations in Space III, pp. 752-762, American Society of Civil Engineers, New York, 1992.

[48] Chambers, J. G., L. A. Taylor, A. Patchen, and D. S. McKay, "Quantitative mineralogical characterization of lunar high- Ti mare basalts and soils for oxygen production", Journal of Geophysical Research, 100, 14,391-14,401, 1995.

[49]   Gibson, M. A., C. W. Knudsen, D. J. Brueneman, C. C. Allen, H. Kanamori, and D. S. McKay, "Reduction of lunar basalt 70035: Oxygen yield and reaction product analysis", *Journal of Geophysical Research, 99*, 10,887-10,897, 1994.

[50]   Allen, C. C., R. V. Morris, and D. S. McKay, "Experimental reduction of lunar mare soil and volcanic glass", *Journal of Geophysical Research, 99*, 23,173 - 23,195, 1994.

[51]   Allen, C. C., R. V. Morris, and D. S. McKay, "Oxygen extraction from lunar soils and pyroclastic glass", submitted *to Journal of Geophysical Research*, 1996.

[52]   Davis, P. A. Jr., "Iron and titanium distribution on the Moon from orbital gamma ray spectrometry with implications for crustal evolutionary models", *Journal of Geophysical Research, 85*, 3209-3224, 1980.

[53]   Feldman, W. C., A. B. Binder, G. S. Hubbard, R. E. Murray Jr., M. C. Miller, and T. H. Prettyman, "The Lunar Prospector gamma-ray spectrometer", *Lunar and Planetary Science XXVII*, 355-356, 1996.

[54]   Lucey, P. G., G. J. Taylor, and E. Malaret, "Abundance and distribution of iron on the Moon", *Science, 268*, 1150-1153, 1995.

[55]   Delano J., "Pristine lunar glasses: Criteria, data and implications", Proc. 16th Lunar Planet. Sci.. Conf., Part 2, J. Geophys. Res., 91, D201-213, 1986.